

See discussions, stats, and author profiles for this publication at: <https://www.researchgate.net/publication/235332937>

Intrarenal metabolomic investigation of chronic kidney disease and its TGF- β 1 mechanism in induced-adenine rats using UPLC Q-TOF/HSMS/MS(E)

ARTICLE *in* JOURNAL OF PROTEOME RESEARCH · FEBRUARY 2013

Impact Factor: 4.25 · DOI: 10.1021/pr3007792

CITATIONS

35

READS

109

7 AUTHORS, INCLUDING:



[Ying-Yong Zhao](#)

Northwest University

108 PUBLICATIONS 1,186 CITATIONS

[SEE PROFILE](#)



[Xian-Long Cheng](#)

National Institutes for Food and Drug Control, ...

65 PUBLICATIONS 694 CITATIONS

[SEE PROFILE](#)



[Feng Wei](#)

National Institutes for Food and Drug Control, ...

66 PUBLICATIONS 618 CITATIONS

[SEE PROFILE](#)

Intrarenal Metabolomic Investigation of Chronic Kidney Disease and its TGF- β 1 Mechanism in Induced-adenine Rats using UPLC Q-TOF/HSMS/MS^E

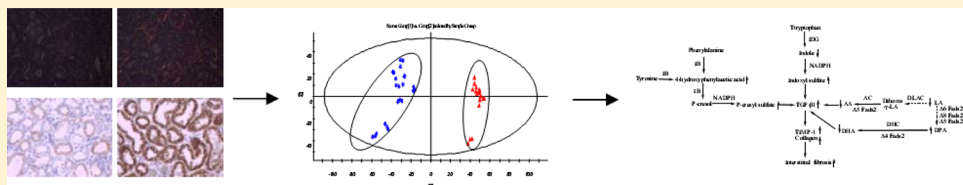
Ying-Yong Zhao,^{*,†} Xian-Long Cheng,[‡] Feng Wei,[‡] Xu Bai,[§] Xiao-Jie Tan,[§] Rui-Chao Lin,[‡] and Qibing Mei^{*,||}

[†]Key Laboratory of Resource Biology and Biotechnology in Western China, Ministry of Education, the College of Life Sciences, Northwest University, No.229 Taibai North Road, Xi'an, Shaanxi 710069, China

[‡]National Institutes for Food and Drug Control, State Food and Drug Administration, No. 2 Tiantan Xili, Beijing, 100050, China

^{||}Department of Pharmacology, School of Pharmacy, the Fourth Military Medical University, Xi'an 710032, China

[§]Waters Technologies (Shanghai) Ltd., No. 1387 Zhangdong Road, Shanghai 201203, China



ABSTRACT: Chronic kidney disease (CKD) is becoming a worldwide public health problem. In this study, a kidney metabolomics method based on the ultra performance liquid chromatography/high-sensitivity mass spectrometry with MS^E data collection technique was undertaken to explore the excretion pattern of low molecular mass metabolites in rat model of adenine-induced chronic renal failure (CRF). Coupled with blood biochemistry and kidney histopathology results, the significant difference in metabolic profiling between the adenine-induced CRF group and the control group by using pattern recognition analysis indicated that changes in global tissue metabolites were occurred. Some significantly changed metabolites like fatty acids, *p*-cresol sulfate, and indoxyl sulfate have been identified. The results showed that the most important CRF-related metabolites were polyunsaturated fatty acids, indoxyl sulfate, and *p*-cresyl sulfate. Indoxyl sulfate and *p*-cresyl sulfate (uremic toxins) were significantly increased in CRF rats. Indoxyl sulfate and *p*-cresyl sulfate stimulate progressive tubulointerstitial fibrosis by increasing the expression of transforming growth factor- β 1 (TGF- β 1). These biochemical changes in tissue metabolites are related to the perturbations of fatty acid metabolism and amino metabolism, which may be helpful to further understand the TGF- β 1 mechanisms of tubulointerstitial fibrosis. This work shows that the metabolomics method is a valuable tool for studying the essence of CKD.

KEYWORDS: chronic kidney disease, metabolomic, ultra performance liquid chromatography, MS^E, TGF- β 1

INTRODUCTION

Chronic kidney disease (CKD) is becoming a worldwide public health problem. At present, approximately 8–10% of individuals in western countries are affected by chronic progressive kidney failure, and diffusion of diabetes and metabolic syndrome within youngsters will even worsen the scenario in the years to come.^{1,2} The kidney's role in acid–base balance, the regulation of plasma volume, and hormone secretion is crucial in sustaining vertebrate homeostasis but can be diminished by many kidney diseases that lead to a loss of organ function. CKD, characterized by a low glomerular filtration rate, is a steady loss of renal function over a period of time. The causes are manifold and include diabetes, hypertension, chronic glomerulonephritis, and tubulointerstitial fibrosis.³ Current assessments of renal function warrant the use of serum creatinine (Scr) and blood urea nitrogen (BUN), and this method has remained unchanged for several decades. It is commonly accepted that these biomarkers display poor

sensitivity and specificity in indicating early arising, acute changes in kidney function and that they do not differentiate between the renal function itself, represented by the functional nephron number, and the extent of active lesions as indicators of active kidney damage.⁴ Knowledge of the complex molecular and pathophysiological mechanisms leading to CKD remains limited, in part because conventional research tools have hampered investigators by restricting their focus to a single or relatively few risk markers at one time.

Metabolomics, as one of the “-omics” technologies involving modern chemical instrumental analysis and chemometrics analysis, is used to characterize the biochemical patterns of the endogenous metabolic composition of biological samples (serum, plasma, urine, tissue), which is ideal for detecting the physiopathological response to a toxin- or disease-inducing

Received: August 18, 2012

Published: December 11, 2012



disturbance or disequilibria in an endogenous metabolic network.^{5–8} In contrast to classical biochemical approaches that often focus on a single metabolite, metabolomics involves the collection of quantitative data on a broad series of metabolites and attempts to gain an overall understanding of metabolism and/or metabolic dynamics associated with conditions of disease and drug exposure.

Recently, an increasing number of publications have described metabonomic studies using various techniques including nuclear magnetic resonance, gas chromatography/mass spectrometry and liquid chromatography coupled with mass spectrometry (LC–MS).⁹ Among the analytical techniques in metabonomic research, LC–MS is recognized as one of the best analytical techniques in selectivity, sensitivity, and reproducibility.^{10,11} Furthermore, among the various LC–MS platforms, ultra performance liquid chromatography mass spectrometry (UPLC–MS) is considered to be suitable for metabolite profiling and metabonomics study, especially for large-scale untargeted metabolic profiling due to its enhanced reproducibility of retention time.^{12,13} In 2005, Wrona et al. introduced the MS^E (where E represents collision energy) technique for the first time.¹⁴ MS^E can provide parallel alternating scans for acquisition at either low collision energy to obtain precursor ion information or ramping of high collision energy to obtain full-scan accurate mass fragment, precursor ion, and neutral loss information.^{15–17}

UPLC–MS has been used to study the serum or urinary metabolites of the animals or patients with chronic renal failure (CRF) and is suitable for analysis *in vivo*.^{13,18,19} Adenine is a nitrogen heterocycle and its final metabolite is uric acid. Normally, adenine is efficiently salvaged by adenine phosphoribosyltransferase and is present at very low levels in blood and urine.^{20,21} In mammalian metabolism, when adenine is present in excess, it becomes a significant substrate for xanthine dehydrogenase, which can oxidize adenine to 2,8-dihydroxyadenine via an 8-hydroxyadenine intermediate.²² Adenine and 2,8-dihydroxyadenine are excreted in urine. However, the very low solubility of 2,8-dihydroxyadenine can lead to its precipitation in the tubules of the kidney.²³ Yokzawa et al. reported a new animal model of CRF induced by an adenine-rich diet. Adenine produces metabolic abnormalities resembling chronic renal insufficiency in humans.²⁴ In the present study, CRF model rats were established by treating the male Sprague–Dawley (SD) rats with adenine.²⁴ A sensitive ultra performance liquid chromatography coupled with quadrupole time-of-flight high-sensitivity mass spectrometry (UPLC Q-TOF/HSMS) with a MS^E data collection technique method was developed for the analysis of endogenous metabolites in rat kidney. Principal component analysis (PCA) and orthogonal partial least-squares-discriminant analysis (OPLS-DA) were performed for investigating the metabolic changes of adenine-induced CRF and normal control rats, and the potential biomarkers were identified accordingly.

MATERIALS AND METHODS

Chemicals and Reagents

Adenine (batch No.: A8626, Purity 99.0%) and formic acid solution (ref BCBB6918, purity 50%) were purchased from Sigma Chemical Co., Ltd. (Sigma Corp., St. Louis, MO). Creatinine (batch No.: 100877–200901, Purity 99.8%) was obtained from the National Institutes for Food and Drug Control (Beijing, China). Transforming growth factor $\beta 1$

(TGF- $\beta 1$) protein was purchased from Santa Cruz Biotechnology Company (Santa Cruz Biotechnology, Inc., CA). LC-grade methanol and acetonitrile were purchased from the Baker Company (Mallinckrodt Baker Inc., Phillipsburg, NJ). Ultra high purity water was prepared using a Milli-Q water purification system (Millipore Corp., Billerica, MA). Other chemicals were of analytical grade and their purity was above 99.5%.

Animals and Sample Collection

The study was conducted in accordance with the Regulations of Experimental Animal Administration issued by the State Committee of Science and Technology of People's Republic of China. All procedures and the care of the rats were in accordance with institutional guidelines for animal use in research. Male SD rats were obtained from the Central Animal Breeding House of Xi'an Jiaotong University (Xi'an, China). They were maintained at a constant humidity (ca. 60%) and temperature (ca. 23 °C) with a light/dark cycle of 12 h.

Male rats underwent an adaptation period of several days, during which they were fed a commercial feed. The rats weighing 190–210 g were divided into 2 groups ($N = 12$ /group) after measuring of body weight. Group 2 was given 200 mg/kg body weight of adenine dissolved with 1% (w/v) gum acacia solution (by gastric gavage, instead of adenine added in food),²⁴ which produced experimental renal failure in the animal for 20-day study periods. Group 1 was similarly given an equal volume of gum acacia solution. Body weight was measured daily for all rats. Rats were anesthetized with 10% urethane, and blood samples were obtained by carotid artery cannula, and the left kidney was harvested after *in situ* cardioperfusion. Then, the removed kidneys were immediately washed with physiological saline and stored at –80 °C for the following histological and metabolomic study.

Determination of Body Weight, Kidney Index and Blood Sample

At the end of the experiment, rats were housed individually in metabolic cages for 24 h urinary collection and the body weight of rats was measured. The kidney weight index was calculated by dividing the kidney weight by the body weight. The kidney length and width indexes were calculated by dividing the kidney length and width by the body weight. Blood parameters were determined by HF-3800 Routine blood analyzer and total cholesterol and triglycerides were measured using an Olympus AU640 automatic analyzer.

Evaluation of Renal Fibrosis

Picro-sirius red staining was used to evaluate the area occupied by collagen fibrils. The kidneys were fixed in 10% buffered formalin for light microscopic examination. After fixation, sections of the kidney were dehydrated with graded ethanol and embedded in paraffin. Sections of 5 μ m of paraffin-embedded tissues were mounted on glass slides, rehydrated with distilled water. Sections were incubated overnight in picro-sirius red solution (1% sirius red in saturated picric acid). Slides were dehydrated and mounted after being placed in 0.01 N HCl for 2 min and examined by polarized light microscopy.

Immunohistochemistry

For histological analysis, the kidneys were fixed in 10% buffered formalin for light microscopic examination. After fixation, sections of the kidney were dehydrated with graded ethanol and embedded in paraffin. Sections of 5 μ m of paraffin-embedded tissues were mounted on glass slides, rehydrated with distilled

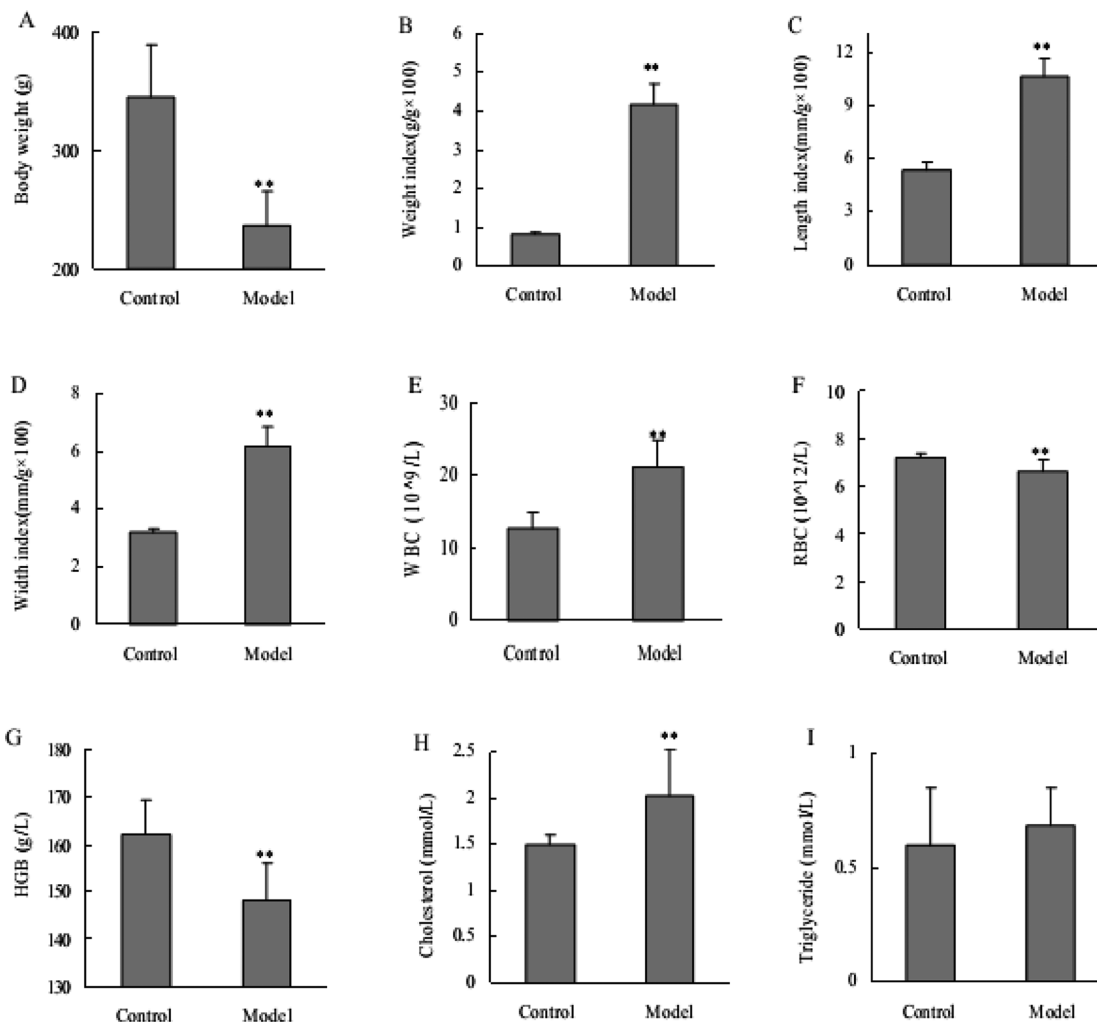


Figure 1. Physical and biochemical parameters comparisons between CRF and control groups. (A) Body weight; (B) kidney weight index; (C) kidney length index; (D) kidney width index; (E) white blood cell count; (F) red blood cell; (G) hemoglobin; (H) cholesterol and (I) triglyceride. The data were expressed as mean \pm SD. **significant difference compared with control groups ($P < 0.01$).

water and the sections were used for immunohistochemistry of TGF- β 1 protein according to the methods described by Shankland et al.²⁵

Sample Preparation

Extraction methods were taken, and in some cases modified, from previous work.^{26–29} Kidney samples (100 mg) were homogenized in 0.5 mL of acetonitrile in an ice bath. Samples were then vortexed for 2 min, and put on ice in between. Following centrifugation (13,000 rpm, 10 min, 4 °C), 300 μ L of supernatant was removed and then lyophilized. Before analysis, the extract was resuspended in 100 μ L acetonitrile/water (4:1) for UPLC analysis.

Chromatographic Separation

The UPLC analysis was performed with a Waters Acquity Ultra Performance LC system (Waters, Milford, MA) equipped with a Waters Xevo G2 QToF MS (Waters MS Technologies, Manchester, UK). Chromatographic separation was carried out at 45 °C on an ACQUITY UPLC HSS T3 column (2.1 mm \times 100 mm, 1.8 μ m, UK). The mobile phase consisted of water (A) and acetonitrile (B), each containing 0.1% formic acid. The optimized UPLC elution conditions were: 0–2.0 min, 1–60% B; 2.0–6.0 min, 60–85% B; 6.0–8.0 min, 85–99% B and 8.0–10.0 min, 99.0–1.0% B. The flow rate was 0.45 mL/min. The

autosampler was maintained at 4 °C. One microliter of sample solution was injected for each run.

Mass Spectrometry

Mass spectrometry was performed on a Xevo G2 QToF (Waters MS Technologies, Manchester, UK), a quadrupole and orthogonal acceleration time-of-flight tandem mass spectrometer. The scan range was from 50 to 1200 m/z . For negative electrospray mode, the capillary and cone voltage were set at 2.5 kV and 45 V, respectively. The desolvation gas was set to 800 L/h at a temperature of 450 °C; the cone gas was set to 30 L/h and the source temperature was set to 120 °C. The mass spectrometry was operated in W optics mode with 12000 resolution using dynamic range extension. The data acquisition rate was set to 0.1 s, with a 0.01 s interscan delay. All analyses were acquired using the lockspray to ensure accuracy and reproducibility. Leucine-enkephalin was used as the lockmass at a concentration of 300 ng/mL and flow rate of 5 μ L/min. Data were collected in continuum mode, the lockspray frequency was set at 10 s, and data were averaged over 10 scans. All the acquisition and analysis of data were controlled by Waters MassLynx v4.1 software.

Data Analysis

The mass data acquired were imported to Markerlynx XS (Waters Corporation, Milford, MA) within the Masslynx software for peak detection and alignment. All of the data were normalized to the summed total ion intensity per chromatogram, and the resultant data matrices were introduced to the EZinfo 2.0 software (Waters Corporation, Milford, MA) for PCA and OPLS-DA. Metabolite peaks were assigned by MS^E analysis or interpreted with available biochemical databases, such as HMDB (<http://www.hmdb.ca/>), ChemSpider (<http://www.chemspider.com/>) and KEGG (<http://www.kegg.com/>). Potential markers were extracted from S-plots constructed following analysis with OPLS-DA, and the markers were chosen based on their contribution to the variation and correlation within the data set. Other statistical analyses were performed using SPSS 11.0 (SPSS Inc., Chicago, IL). Significant differences were considered significant when test *p* values were less than 0.05.

RESULTS AND DISCUSSION

Basic Physical and Biochemical Parameters

Figure 1 shows the parameters of body weight, kidney index and blood sample in the control and CRF rats. Body weight was markedly decreased in the adenine-induced CRF group compared with that in the control group and arrived at statistical significance (*p* < 0.01). Similarly, compared with the control group, weight index (Figure 1B), length index (Figure 1C) and width index (Figure 1D) of kidney was markedly increased in the adenine-induced CRF group (*p* < 0.01). A remarkable increase in white blood cell count (Figure 1E) and a remarkable decrease in red blood cell (Figure 1F) and hemoglobin (Figure 1G) were revealed in the blood parameters of the adenine-induced CRF group compared with the control group. These blood parameters showed that adenine can cause anemia symptom. After day 20, blood samples were collected and serum cholesterol and triglyceride were determined. The results are given in Figure 1H and I. Cholesterol were in higher concentration in the adenine-induced CRF group than in the control group (*p* < 0.01). The triglyceride level in the adenine-induced CRF rats was slightly increased beyond the normal level, but did not arrive at statistical significance (Figure 1I). In our previous results, the levels of SCr and BUN in the adenine-induced CRF rats were markedly increased beyond the normal level.¹⁹ These results demonstrate that the rat model exhibited typical pathologic features associated with CRF.

Picro-sirius Red Staining

Picro-sirius red staining is one of the best understood techniques of collagen histochemistry. The birefringence is highly specific for collagen. In bright-field microscopy, collagen is red on a pale yellow background. When examined through crossed polars the larger collagen fibers are bright yellow or orange, and the thinner ones, including reticular fibers, are green. Figure 2 shows histologic findings by picro-sirius red staining of transverse kidney sections in the control group (Figure 2A) and CRF group (Figure 2B). In the CRF rats, periarteriolar fibrosis, tubulointerstitial fibrosis, and intra-glomerular fibrosis were markedly increased in the kidney from the adenine-induced CRF rats.

TGF- β 1 Immunohistochemistry

TGF- β 1 is a member of a family of polypeptide factors that control proliferation, differentiation, chemotaxis, and other

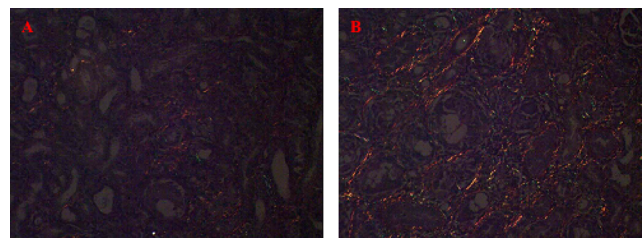


Figure 2. Histologic findings by picro-sirius red staining of transverse kidney sections in the (A) control and (B) CRF rats. Magnification, $\times 200$.

functions in many cell types. TGF- β 1 has been shown to inhibit many immunologic functions. Figure 3 shows TGF- β 1

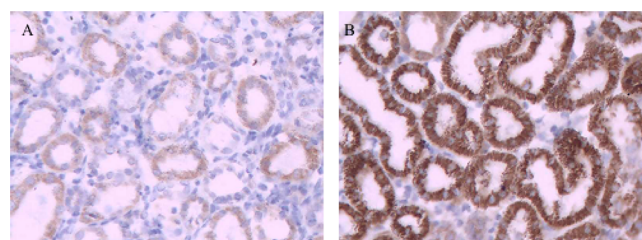


Figure 3. Immunohistochemical findings by antitransforming growth factor- β 1 (TGF- β 1) antibody in the (A) control group and (B) CRF group of rat kidneys. Magnification, $\times 400$.

immunostaining in the kidney from the control group (Figure 3A) and CRF group (Figure 3B). In control kidney sections, TGF- β 1 protein expression was detected in some glomeruli and tubulointerstitiums. TGF- β 1 protein expression was markedly increased in the glomeruli and tubulointerstitiums from the adenine-induced CRF rats.

Optimization of Chromatographic Conditions

The complexity of the tissue sample makes the separation very difficult, consequently results in severe ion suppression. The selection of UPLC columns with high separation efficiency is a prerequisite. To date, silica columns for UPLC in normal phase have still to be developed, and therefore the studied metabolites were resolved in the reversed or “aqueous normal” phase. Two columns were investigated for this purpose. These were the BEH (ethylene bridged hybrid) C18 column (2.1 mm \times 100 mm, 1.7 μ m, Waters) and the HSS (high strength silica) T3 column (2.1 mm \times 100 mm, 1.8 μ m, Waters). The BEH C18 column is the universal column choice for most UPLC separations. The HSS T3 column, 100% silica particle, is used to retain and separate smaller, more water-soluble polar organic compounds than the BEH C18 column. The HSS T3 column could be practical for the separation of xanthophylls since it was designed for greater retention of polar compounds.³⁰ The HSS T3 column has been proven to provide higher retention for the polar analytes and to obtain a good chromatographic separation.

Tissue samples were measured both in the positive ion mode and in the negative ion mode. We observed that higher noise and matrix effect in the positive ion mode resulted in a higher baseline, which led to the neglect of some metabolites of low abundance and the concomitance of multiple adduction ions. Relatively, adequate information of metabolites could be detected, and most usually formed dominating quasi-molecular ion [M - H]⁻ or [M + HCOO]⁻ with a higher signal/noise in

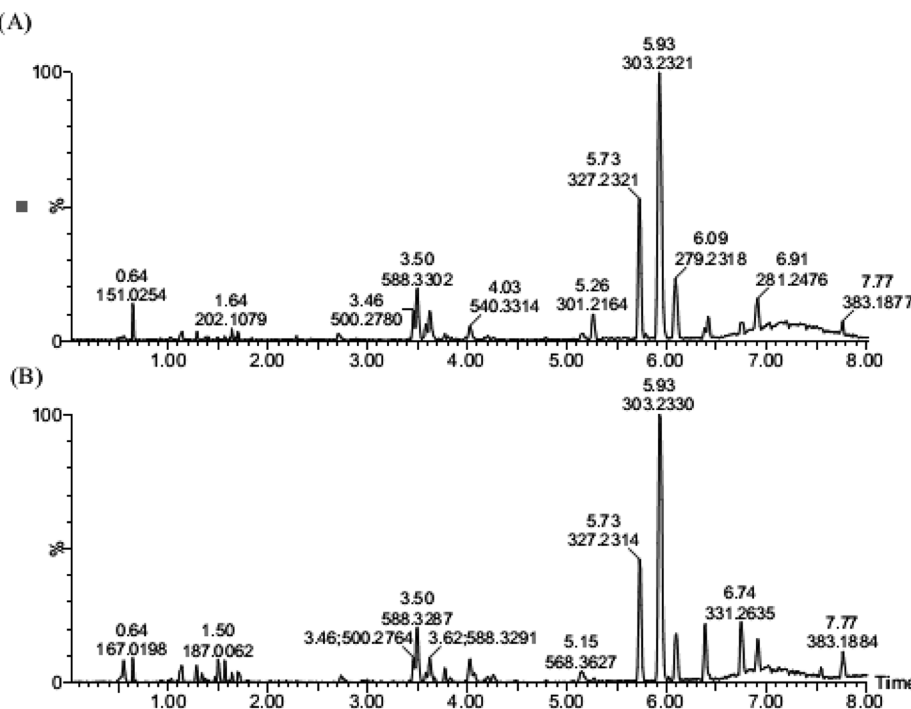


Figure 4. Base peak intensity (BPI) chromatograms obtained from tissue sample in (A) control group and (B) CRF group.

the negative ion mode. This may be due to the phospholipids presented in the samples. Phospholipids are known to be prone to form adduct ions in positive ion mode and may depress the ionization of metabolites in tissue. Therefore, considering maximization of the number of detectable metabolites and the quality of data acquired, negative ion mode was applied for final analysis.

To obtain chromatograms with good resolution, acetonitrile–water and methanol–water were investigated and the former was chosen. Various additives of formic acid, acetic acid and ammonium acetate were investigated, and 0.1% formic acid gave the best separation and peak shape. Therefore, the mobile phase consisted of water (0.1% formic acid) and acetonitrile (0.1% formic acid) using a gradient elution. To minimize thermal degradation of the metabolites while waiting to be analyzed, the autosampler compartment was set at 4 °C throughout the analysis. Here, metabolic profiling of tissue samples was acquired using UPLC–MS system in negative ESI mode. Figure 4 presents the typical negative base peak intensity (BPI) chromatograms of tissue samples from the control and CRF groups.

Validation of UPLC–MS Conditions

In the assessment of system repeatability, extracted ion chromatographic peaks of seven ions in negative ion mode were selected. The relative standard deviations (RSD) of retention times and peak areas of seven selected ions in six batches of kidney samples were below 0.48 and 3.4%. The assessment data acquired from QC sample also showed good system stability. The RSD of retention times and peak areas of seven selected ions were below 0.83 and 3.1%. The developed method had a good repeatability and stability.

Multivariate Analysis of UPLC–MS Data

Metabolic profiling of tissue samples was acquired using UPLC Q-TOF/HSMS and MS^E data collection technique system in the negative ESI mode. The BPI chromatograms of tissue

samples from the control group and CRF group are shown in Figure 4. The PCA and OPLS-DA analysis were performed on the tissue metabolite concentrations from the control group and CRF group. According to UPLC–MS data, 2193 peaks of negative ions were detected and processed by MarkerLynx XS using the same acquisition method. The metabolic patterns of kidney in rats of each group during the 20-day study periods after experiment were plotted by the PCA in the negative ion mode (Figure 5). The parameters for the classification from the EZinfo 2.0 software were $R^2Y = 0.512$ and $Q^2 = 0.445$, which are good to fitness and prediction, respectively. In the kidney PCA score plot, the CRF group and control group were separated clearly, indicating that the CRF model was successfully reproduced in negative ion mode. This indicates that adenine-induced CRF rats have significantly altered renal metabolism, and hence the altered profiling of renal metabolites could reflect the changes in renal metabolism affected by adenine.

Identification of Potential Biomarkers

In today's metabolomics research, the biggest challenge is the identification of potential biomarker obtained from comparative samples, particularly when they are novel and published work on the compound class is unavailable or prior information is lacking otherwise. All the detected ions were arranged in descending order according to Variable Importance in the Projection (VIP) values, which reflect the influence of each metabolite in the two groups. The more the variable deviates from the origin, the higher the value of VIP will be obtained. When VIP > 1.0, the variable can be considered as a contributor for the classification of control group and CRF group. The S-plot (shown in Figure 5B), a further loading plot, is a visual method that can be used for selection of biomarkers. Variables that are farthest from the origin in the S-plot are selected as potential biomarkers. Structure identification was performed according to their molecular ion masses, MS^E fragments and i-FIT value comparing with authentic standards or literatures and

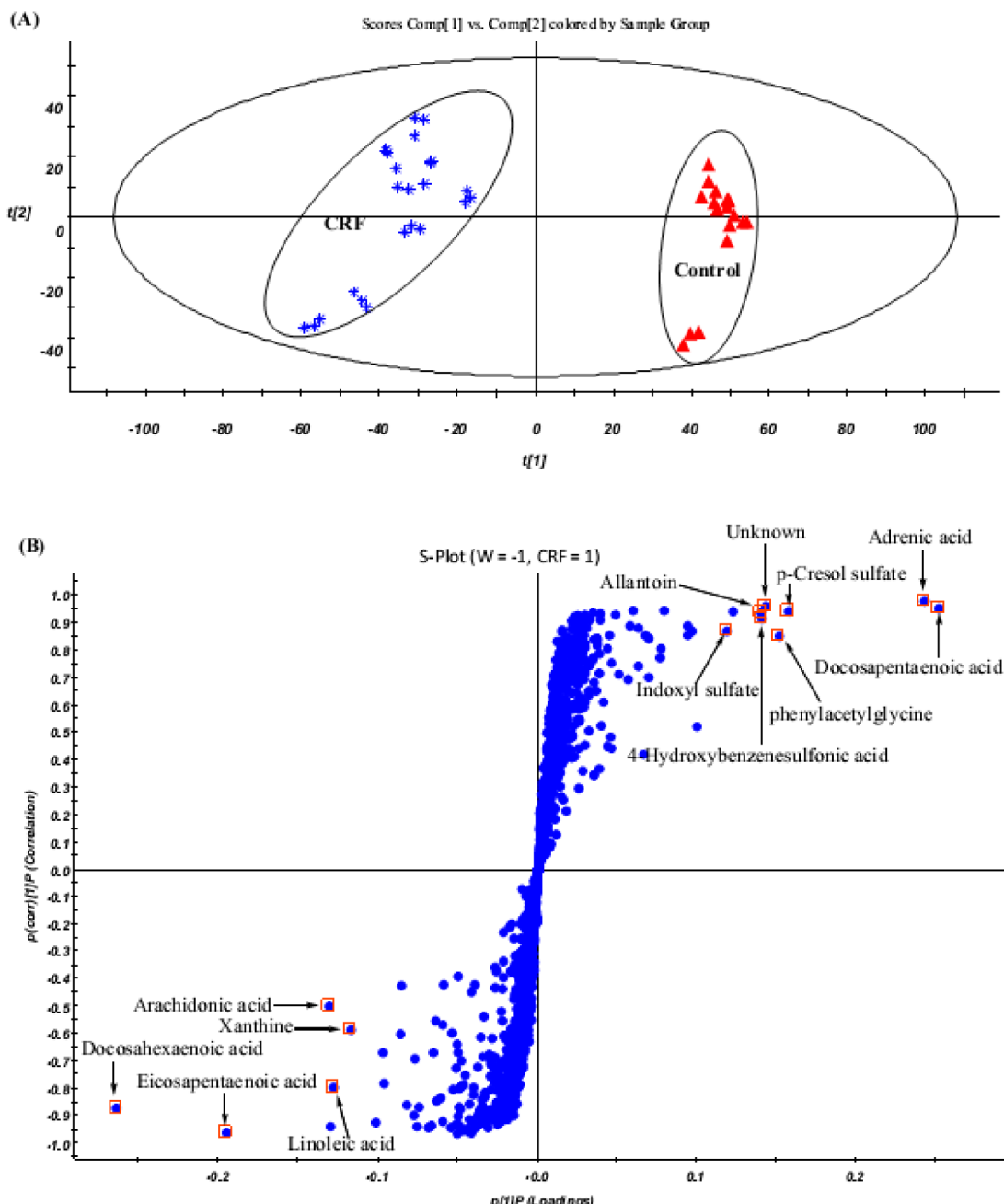


Figure 5. (A) PCA score plot based on the kidney metabolic profiling of the adenine-induced CRF group (*) and control group (▲); (B) S-plot used in biomarkers selection. The variables marked (□) are the metabolites selected as potential biomarkers.

database resources. First, MassLynx i-FIT algorithm is used to screen suggested elemental compositions according to the following procedure: the calculated mass, mass deviation (mDa and ppm), double bond equivalent, formula, and i-FIT value were calculated with the selected m/z ions. The lower the i-FIT value, the better the fit. The lower i-FIT value and smaller mass deviation indicate a more accurate elemental composition. Second, the structure information was obtained by searching freely accessible databases of HMDB (<http://www.hmdb.ca/>), Chemspider (<http://www.chemspider.com/>) and KEGG (<http://www.kegg.com/>) utilizing the accurate MS data, MS^E fragments, molecular weights and elemental compositions. As a result, 12 metabolites were identified on the basis of accurate elemental compositions and context of retention time with available databases. Third, as compensation, 5 of them were

confirmed with available reference standards by matching their retention time and accurate mass measurement. Table 1 shows 12 compounds were tentatively identified. Four of the identified biomarkers' extracted ion chromatogram, MS and MS^E (docosahexaenoic acid, *p*-cresol sulfate, phenylacetyl glycine and indoxyl sulfate), are shown in Figure 6. However, it should be noted that the metabolite ion at t_m/z 7.54_359.2941 was unidentified in the present experiment. Analyses of high-resolution MS data and isotope patterns of the ion matched an elemental composition of $C_{24}H_{40}O_2$, which indicated that the compound belonged to fatty acid. Further study on this potential biomarker is needed for its structure elucidation.

Table 1. Twelve Biomarkers of CRF Detected by UPLC Q-TOF/MS in Negative Ion Modes

no	<i>t</i> _R (min)	metabolite	elemental composition (mDa, i-FIT) ^a	<i>m/z</i>	MS ^E	losses	trend ^b	related pathway
1	5.73	Docosahexaenoic acid	0.8, 0.0, C ₂₂ H ₃₁ O ₂	327.2316	283.2426 229.1987	-CO ₂ -C ₅ H ₆ O ₂	↓***	Fatty acid metabolism
2	6.39	Docosapentaenoic acid	0.8, 0.1, C ₂₂ H ₃₃ O ₂	329.2473	285.2582 231.2154	-CO ₂ -C ₅ H ₆ O ₂	↑***	Fatty acid metabolism
3	6.75	Adrenic acid	1.2, 0.2, C ₂₂ H ₃₅ O ₂	331.2630	287.2698	-CO ₂	↑***	Fatty acid metabolism
4	5.26	Eicosapentaenoic acid	0.8, 0.0, C ₂₀ H ₂₉ O ₂	301.2160	257.2171 203.2018	-CO ₂ -C ₅ H ₆ O ₂	↓***	Fatty acid metabolism
5	1.50	<i>p</i> -Cresol sulfate	1.1, 0.7, C ₇ H ₇ O ₄ S	187.0059	107.0494 79.9951	-SO ₃ -C ₇ H ₇ O	↑***	Tryptophan metabolism
6	1.56	Phenylacetylglycine	1.8, 1.0, C ₈ H ₈ N ₈ OP	192.0655	146.9644 74.0236	-C ₂ HO ₂ -C ₈ H ₆ O	↑***	Phenylalanine metabolism
7	7.54	Unknown	1.8, 0.2, C ₂₄ H ₃₉ O ₂	359.2941	-	-	↑***	-
8	5.93	Arachidonic acid	0.7, 0.0, C ₂₀ H ₃₁ O ₂	303.2317	259.2418 205.1942	-CO ₂ -C ₅ H ₆ O ₂	↓*	Prostaglandin and leukotriene metabolism
9	0.53	Allantoin	0.8, 0.8, C ₄ H ₅ N ₄ O ₃	157.0356	128.9587 114.0306	-CO -CHON	↑***	Purine metabolism
10	1.28	4-Hydroxybenzenesulfonic acid	1.8, 0.1, C ₇ H ₄ N ₄ S	172.9904	93.0339	-SO ₃	↑***	-
11	6.09	Linoleic acid	0.6, 0.7, C ₁₈ H ₃₁ O ₂	279.2318	251.1989	-CO	↓***	Fatty acid metabolism
12	0.64	Xanthine	0.0, 1.4, C ₅ H ₅ N ₄ O ₂	151.0251	134.0301	-NH ₃	↓***	Purine metabolism
13	1.34	Indoxyl sulfate	0.7, 0.3, C ₈ H ₅ NO ₄ S	212.0011	132.0488 79.9556	-SO ₃ -C ₈ H ₆ NO	↑***	Tryptophan metabolism

^amDa, Difference from the exact mass; i-FIT, The i-FIT is meaning the correctness of isotope patterns of elemental composition. The lower i-FIT normalized values mean high precision of the elemental composition. ^bChange trend of CRF rats vs control rats. The levels of potential biomarkers were labeled with (↓) down-regulated and (↑) up-regulated. **p* < 0.05, ***p* < 0.01 and ****p* < 0.001.

Biochemical Interpretation in Adenine-induced CRF Rats

Under certain situations, the differences of some metabolic pathways between human and animals make it difficult to predict toxicology effect on human being with metabolomics study results using animal model. Therefore, it is tremendously important for metabolomics investigation to choose suitable experimental animals which are close to human in genotype, phenotype and metabolic type. According to Yokzawa et al., excretion of nitrogen compounds is suppressed by renal tubular occlusion due to 2,8-dihydroxyadenine. This, in turn, leads to accumulation of urea nitrogen and creatinine in the blood, with a resultant increase of various guanidine compounds.²⁴ These metabolic changes, which are widespread in human and other mammalian including rodents, have been successfully applied in many medical studies to demonstrate drug's toxicological or pharmacological action. However, for the future metabolomics study on certain complicated physiological and pathological mechanisms, experimental animals having closer genetic relationships with humans such as primates and humanized animals should be chosen.

Serum and urinary metabolic profiling have recently been exploited for the studies of the pathophysiology of CRF and some metabolites have been identified in CRF patients or CRF rats previously.^{13,18,19,31–34} However, to the best of our knowledge, a comprehensive profile of kidney metabolites and the difference in metabolic pattern have not been previously reported, particularly by exploiting UPLC-based metabolomics. A relatively new approach of untargeted profiling, which identifies as many metabolites as possible in a UPLC Q-TOF/HSMS and a MS^E data collection technique, was used in our study to understand the changes in metabolic responses of the kidney to adenine-induced CRF at the biochemical level.

Differences in the levels of metabolites between the CRF group and control group were compared using multivariate analysis, such as PCA and OPLS-DA. The metabolic profile and multivariate pattern recognition approach we used permitted us to observe a broad range of metabolites simultaneously, the concentrations of which could be changed by biologic stimuli or certain disease conditions. Since metabolites can be regulated through a number of metabolic pathways, an investigation of the overall features rather than of several select metabolites enabled us to understand the underlying pathophysiological status more comprehensively.

To investigate the change of the potential biomarkers in the kidney of adenine-induced CRF rats, we compared the relative intensity of putative potential biomarkers in kidney (Figure 7) in the normal control and adenine-induced CRF rats. In the renal tissue of CRF rats, concentrations of docosapentaenoic acid, adrenic acid, *p*-cresol sulfate, phenylacetylglycine, allantoin, 4-hydroxybenzenesulfonic acid and indoxyl sulfate were all up-regulated, but docosahexaenoic acid, eicosapentaenoic acid, arachidonic acid, linoleic acid and xanthine were down-regulated. These metabolites mentioned above might play important roles in the metabolic changes of adenine-induced CRF rats.

In additional, an OPLS-DA loading plot was generated (Figure 8). The loading plot represented which metabolites were quantitatively higher or lower in adenine-induced CRF groups compared with control groups. Levels of metabolites such as allantoin, 4-hydroxybenzenesulfonic acid, *p*-cresol sulfate, phenylacetylglycine, indoxyl sulfate, arachidonic acid, docosapentaenoic acid and adrenic acid were significantly increased in adenine-induced groups, whereas the levels of xanthine, linoleic acid, eicosapentaenoic acid and docosahexaenoic acid were decreased. Renal metabolites responsible for

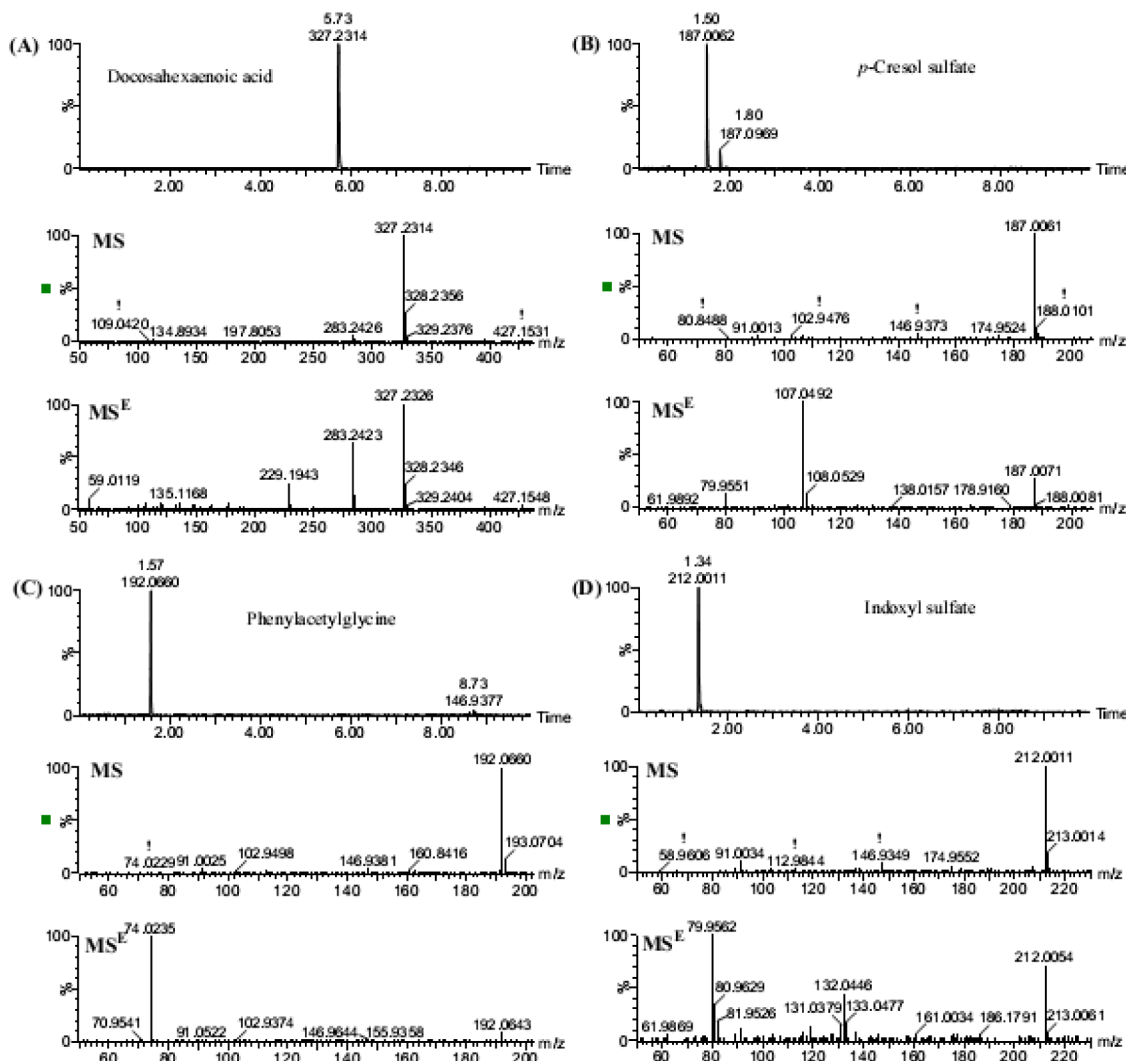


Figure 6. Extracted ion chromatogram, MS and MS^E of (A) docosahexaenoic acid, (B) p-cresol sulfate, (C) phenylacetylglycine and (D) indoxyl sulfate in negative ionization mode.

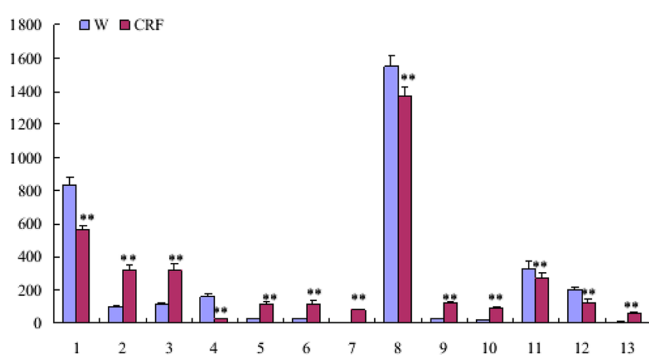


Figure 7. Comparison of the relative intensity of putative potential biomarkers in the normal control and adenine-induced CRF rats.

the observed difference between adenine-induced CRF and control rats are summarized in Table 1.

Lipid metabolism has a key role in CKD, which has been demonstrated by many studies.^{35–38} Lipid-based metabolites play an important role in many biochemistry reactions and are related to many biological functions. In this study, it was found that the most important CRF-related metabolites were polyunsaturated fatty acids (PUFAs). PUFAs are reported to

be associated with atherosclerotic and inflammatory diseases because they are the major components of the cytoplasmic membrane and the precursor fatty acids for prostaglandins and leukotrienes.³⁹

The changes of these fatty acids were quite different. Concentrations of docosapentaenoic acid and adrenic acid were both up-regulated, but docosahexaenoic acid, eicosapentaenoic acid, arachidonic acid and linoleic acid were down-regulated. Nakamura et al. reported docosahexaenoic acid, eicosapentaenoic acid and linoleic acid in hemodialysis patients were significantly lower than those in CKD patients.⁴⁰ A highly significant decrease of γ -linolenic and arachidonic acids was detected in CKD patients as compared to controls, while linoleic acid was elevated in CKD patients, however this elevation was statistically insignificant when compared to the control group.⁴¹ The long chain n-6 fatty acids γ -linolenic and arachidonic acids are present in insufficient amounts in plasma of CKD patients and such insufficiency increases with the severity of the kidney disease confirming the role of impaired n-6 PUFAs metabolism in the development and progression of CKD. Thus, High dietary intake of n-6 fatty acids (mainly γ -linolenic acid) could be recommended as a new therapeutic strategy in CKD patients aiming at interrupting the irreversible

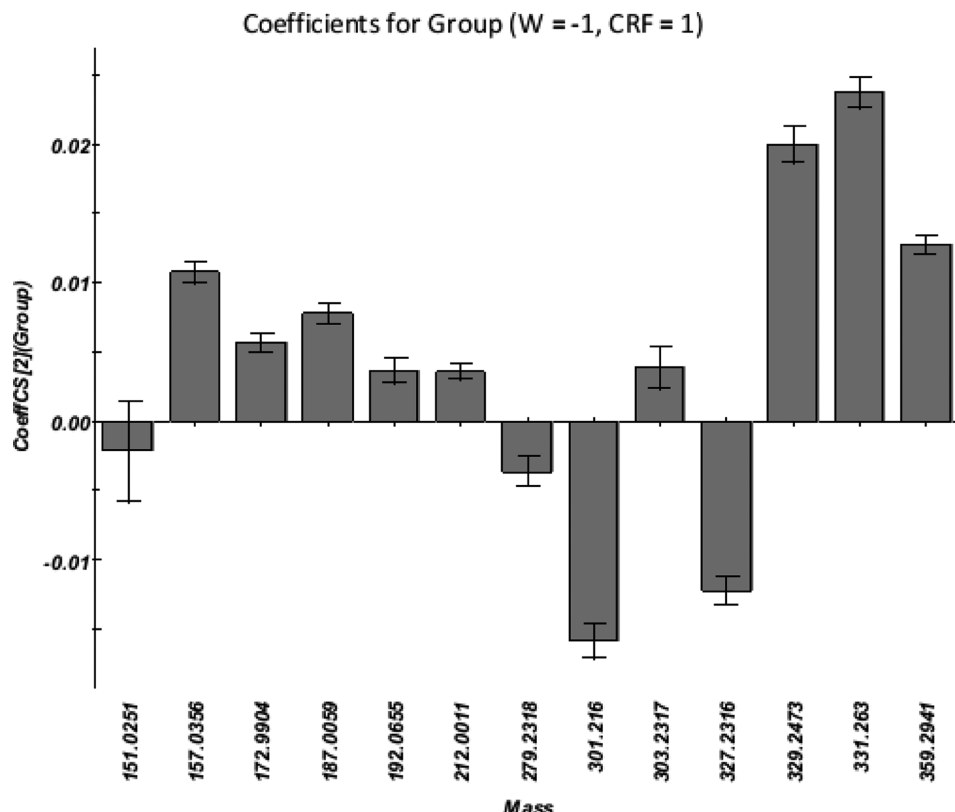


Figure 8. OPLS-DA loading plot in negative ion mode from control group and adenine-induced CRF group. The loading plots represent which metabolites are quantitatively higher or lower in adenine-induced CRF group compared with control group.

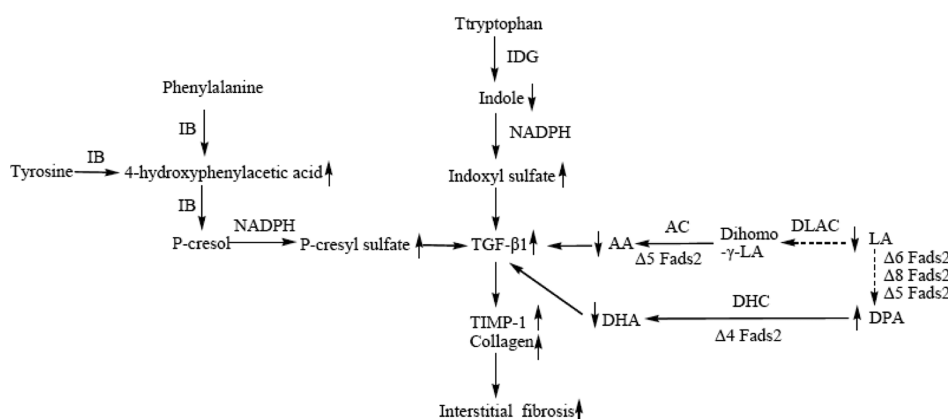


Figure 9. Network of 12 identified biomarkers according to the KEGG pathway database. AA, arachidonic acid; LA, linoleic acid; DHA, docosahexaenoic acid; DAP, docosapentaenoic acid; IB, intestinal bacteria; TPBD, tryptophan 2,3-dioxygenase; DLAC, dihomo- γ -linolenoyl-CoA; AC, arachidonoyl-CoA; DHC, docosahexaenoyl-CoA; IDG, indole 2,3-dioxygenase; NADPH, nicotinamide adenine dinucleotide 2'-phosphate reduced tetrasodium salt.

process of renal fibrosis and ameliorating chronic renal injury. A relationship between PUFAs and renal inflammation and fibrosis, crucial stages in CKD, has been studied (Figure 9). The mechanisms by which PUFAs can favorably interfere with some stages of renal fibrosis, characterized by mesangial cell activation and proliferation and extracellular matrix production, include the activation of intracellular pathways leading to the regulation of the production of profibrotic and antifibrotic as well as of pro- and anti-inflammatory factors.⁴² The addition of arachidonic acid to mesangial cell cultures induced a significant up-regulation of TGF β , fibronectin (FN), connective tissue growth factor (CTGF) and type IV collagen (COLIV)

expression, similar to that induced by angiotensin II, while eicosapentaenoic acid and docosahexaenoic acid had no stimulatory effects. On the contrary, the coexposure of cells to eicosapentaenoic acid or docosahexaenoic acid suppressed the angiotensin II- and arachidonic acid-induced up-regulation of TGF β , FN, CTGF, and COLIV.⁴³

The kidney levels of indoxyl sulfate, *p*-cresyl sulfate and 4-hydroxybenzenesulfonic acid were significantly increased in CRF rats, due to reduced renal clearance of these metabolites. Indoxyl sulfate and *p*-cresyl sulfate have been recognized to be accumulated in uremic serum as albumin-bound uremic retention solutes. Indoxyl sulfate is a metabolite of the

tryptophan. Indoxyl sulfate is a circulating uremic toxin stimulating glomerular sclerosis and interstitial fibrosis and increasing the rate of progression of renal failure.⁴⁴ The administration of indoxyl sulfate to CRF rats promoted the progression of CRF, accompanied by increased gene expression of TGF- β 1, tissue inhibitor of metalloproteinase 1 (TIMP-1) and pro α 1(I) collagen (Figure 9).^{45–47} In plasma, indoxyl sulfate is a protein-bound uremic solute that induces endothelial dysfunction by inhibiting endothelial proliferation and migration in vitro. *p*-Cresyl sulfate is the sulfate conjugates of *p*-cresol, which is produced by intestinal bacteria from tyrosine through 4-hydroxyphenylacetic acid (Figure 9). *p*-Cresol sulfate is a small protein-bound molecule that is poorly cleared with dialysis. *p*-Cresyl sulfate was accumulated in the plasma from hemodialysis patients.⁴⁸ *p*-Cresyl sulfate shows a pro-inflammatory effect on leucocytes.⁴⁹ Indoxyl sulfate and *p*-cresyl sulfate were 93 and 94% bound to albumin, respectively. Increasing evidence shows that level of serum uremic toxins predicts progressive renal injury in patients with CKD.^{50,51} The present study added new evidence that uremic toxins (indoxyl sulfate, *p*-cresyl sulfate, etc.) also significantly increased in CRF and correlated with the severity of renal injury and tubulointerstitial damage. Normally, uremic toxins are mainly produced by liver and/or gastrointestinal flora metabolism,⁵² and eliminated primarily from plasma via active kidney tubular secretion.⁵³ Once the kidney becomes injured, elimination of indoxyl sulfate and *p*-cresyl sulfate is impaired, which results in higher levels of uremic toxins in plasma and may cause corresponding increase of uremic toxins in renal cells. Intrarenal indoxyl sulfate and *p*-cresyl sulfate level in CRF model group were increased by 7 and 4 times compared with control group, while indoxyl sulfate and *p*-cresyl sulfate were not found in serum as reported by a previous study.¹³ These experimental results suggested that the extent of increase of uremic toxins in kidney tissue of CRF rats might be largely higher than that in serum. This obvious disagreement indicates that the increase in intrarenal uremic toxins is most likely to be the consequence of their accumulation when blood flowed through the kidney. An evidence that indoxyl sulfate was found accumulated in the tubular cells by immunohistochemistry method in CRF patients also suggests that the accumulation of uremic toxins might just occur in kidney tubular cells.⁵⁴

Phenylacetyl glycine is a metabolite of phenylalanine by gut microflora.⁵² In this research, adenine caused changes in the concentration of metabolites related to the gut microflora, which strongly suggests that there are variations in the gut microflora in response to adenine administration. Xanthine is an intermediate in the degradation of adenosine monophosphate to uric acid, being formed by oxidation of hypoxanthine. Uric acid is normally excreted into urine and accumulates in uremic serum. The accumulation of uric acid in uremic serum may lead to an elevation of the serum xanthosine level. The serum level of xanthosine is increased in undialyzed patients with CRF and in patients undergoing hemodialysis and continuous ambulatory peritoneal dialysis.⁵⁵

In this study, allantoin was significantly increased in the adenine-induced CRF group compared with the control group. Allantoin is a product of oxidation of uric acid by purine catabolism. It is the predominant means by which nitrogenous waste is excreted in the urine of most mammals except humans and higher apes.⁵⁶ The literature has reported that uric acid injected intravenously into a dog was converted into allantoin within two hours.⁵⁶ However, uric acid is excreted instead of

allantoin in humans and higher apes. The presence of allantoin in the urine can be an indication of microbial overgrowth or it can be created via nonenzymatic means through high levels of reactive oxygen species.⁵⁷ Accumulating evidence has demonstrated that uric acid is oxidized by reactive oxygen species mainly to allantoin^{58,59} and allantoin is used as a marker of oxidative stress, which is related to renal damage.^{60–63}

CONCLUSIONS

A metabonomics approach based on UPLC Q-TOF/HSMS with MS^E data collection technique and chemometrics method has been developed to study the specific physiopathologic state of adenine-induced CRF rats. With the PCA, a clear separation of model group and control group was achieved. Furthermore, 12 potential biomarkers like polyunsaturated fatty acids, *p*-cresol sulfate, phenylacetyl glycine, allantoin and indoxyl sulfate for adenine-induced CRF rats were identified and were correlated with progressive renal injury. Combined with biochemistry and histopathology results, the changes in kidney metabolites indicated the perturbations of fatty acid metabolism and amino acid metabolism are related to CRF metabolic pathways. These results further supported the association of organic toxins with the progression of CRF, which may be helpful to further understand the TGF- β 1 mechanisms of tubulointerstitial fibrosis. MS^E can acquire MS fragment information without the need for sample reinjection, and in the subsequent data processing available information on fragmentation pathways, neutral losses and diagnostic precursor allowed us to identify biomarkers in a relatively fast and efficient manner.

AUTHOR INFORMATION

Corresponding Author

*Y.-Y.Z., Tel +86 29 88304569; Fax +86 29 88304368; E-mail: zyy@nwu.edu.cn; zhaoyybr@163.com. Q.M., Tel +86 29 84779212; Fax +86 29 84774552; E-mail: qbmei@fmmu.edu.cn.

Notes

The authors declare no competing financial interest.

ACKNOWLEDGMENTS

This study was supported in part by grants from the National Scientific Foundation of China (Nos. 81001622, 81073029), Innovative Research Team in University of Ministry of Education of China (No. IRT1174), the project “As a Major New Drug to Create a Major National Science and Technology Special” (No. 2011ZX09401-308-034) from the Ministry of Science and Technology of the People’s Republic of China and the Technology Research Program from Shaanxi Provincial Science and Technology Department (No. 2011K12-69).

ABBREVIATIONS

CKD, chronic kidney disease; CRF, chronic renal failure; TGF- β 1, transforming growth factor- β 1; UPLC Q-TOF/HSMS, ultra performance liquid chromatography coupled with quadrupole time-of-flight high-sensitivity mass spectrometry; MS^E, mass spectrometry^{ENERGY}; SCr, serum creatinine; BUN, blood urea nitrogen; PCA, principal component analysis; OPLS-DA, orthogonal partial least-squares-discriminant analysis; SD, Sprague–Dawley; RSD, relative standard deviations; BPI, base peak intensity; VIP, variable importance in the projection; PUFAs, polyunsaturated fatty acids; FN, fibronectin; CTGF,

connective tissue growth factor; COLIV, type IV collagen; TIMP-1, tissue inhibitor of metalloproteinase 1

■ REFERENCES

- (1) Lameire, N.; Jager, K.; Van, Biesen, W.; de Bacquer, D.; Vanholder, R. Chronic kidney disease: a European perspective. *Kidney Int.* **2005**, *99*, S30–38.
- (2) Levey, A. S.; Atkins, R.; Coresh, J.; Cohen, E. P.; Collins, A. J.; Eckardt, K. U.; Nahas, M. E.; Jaber, B. L.; Jadoul, M.; Levin, A.; Powe, N. R.; Rossert, J.; Wheeler, D. C.; Lameire, N.; Eknoyan, G. Chronic kidney disease as a global public health problem: approaches and initiatives—a position statement from Kidney Disease Improving Global Outcomes. *Kidney Int.* **2007**, *72*, 247–259.
- (3) Meguid, E. L.; Nahas, A.; Bello, A. K. Chronic kidney disease: the global challenge. *Lancet* **2005**, *365*, 331–340.
- (4) Mori, K.; Nakao, K. Neutrophil gelatinase-associated lipocalin as the real-time indicator of active kidney damage. *Kidney Int.* **2007**, *71*, 967–970.
- (5) Ekman, D. R.; Keun, H. C.; Eads, C. D.; Furnish, C. M.; Rockett, J. C.; Dix, D. J. Metabolomic evaluation of rat liver and testis to characterize the toxicity of triazole fungicides. *Metabolomics* **2006**, *2*, 63–73.
- (6) Yin, P.; Mohemaiti, P.; Chen, J.; Zhao, X.; Lu, X.; Yimiti, A.; Upur, H.; Xu, G. Serum metabolic profiling of abnormal savda by liquid chromatography/mass spectrometry. *J. Chromatogr., B* **2008**, *871*, 322–327.
- (7) Holmes, E.; Cloarec, O.; Nicholson, J. K. Probing latent biomarker signatures and in vivo pathway activity in experimental disease states via statistical total correlation spectroscopy (STOCSY) of biofluids: application to $HgCl_2$ toxicity. *J. Proteome Res.* **2006**, *5*, 1313–1320.
- (8) Kellert, M.; Wagner, S.; Lutz, U.; Lutz, W. K. Biomarkers of furan exposure by metabolic profiling of rat urine with liquid chromatography-tandem mass spectrometry and principal component analysis. *Chem. Res. Toxicol.* **2008**, *21*, 761–768.
- (9) Lao, Y. M.; Jiang, J. G.; Yan, L. Application of metabolomic analytical techniques in the modernization and toxicology research of traditional Chinese medicine. *Br. J. Pharmacol.* **2009**, *157*, 1128–1141.
- (10) Aurélie, R.; Dominique, L.; Christophe, J.; Jean-François, H. Applications of liquid chromatography coupled to mass spectrometry-based metabolomics in clinical chemistry and toxicology: A review. *Clin. Biochem.* **2011**, *44*, 119–135.
- (11) Theodoridis, G.; Gika, H. G.; Wilson, I. D. LC-MS-based methodology for global metabolite profiling in metabolomics/metabolomics. *Trend. Anal. Chem.* **2008**, *27*, 251–260.
- (12) Fukui, Y.; Kato, M.; Inoue, Y.; Matsubara, A.; Itoh, K. A metabolomic approach identifies human urinary phenylacetylglutamine as a novel marker of interstitial cystitis. *J. Chromatogr., B* **2009**, *877*, 3806–3812.
- (13) Zhao, Y. Y.; Cheng, X. L.; Wei, F.; Xiao, X. Y.; Sun, W. J.; Zhang, Y. M.; Lin, R. C. Serum metabolomics study of adenine-induced chronic renal failure rat by ultra performance liquid chromatography coupled with quadrupole time-of-flight mass spectrometry. *Biomarkers* **2012**, *17*, 48–55.
- (14) Wrona, M.; Mauriala, T.; Bateman, K. P.; Mortishire-Smith, R. J.; O'Connor, D. 'All-in-One' analysis for metabolite identification using liquid chromatography/hybrid quadrupole time-of-flight mass spectrometry with collision energy switching. *Rapid Commun. Mass Spectrom.* **2005**, *19*, 2597–2602.
- (15) Kevin, P. B.; Jose, C. P.; Mark, W.; John, P. S.; Kate, Y.; Renata, O.; Deborah, A. N. G. MS^E with mass defect filtering for in vitro and in vivo metabolite identification. *Rapid Commun. Mass Spectrom.* **2007**, *21*, 1485–1496.
- (16) Rainville, P. D.; Stumpf, C. J.; Shockcor, J. P.; Plumb, R. S.; Nicholson, J. K. Novel application of reversed-phase UPLC-oaTOFMS for lipid analysis in complex biological mixture: a new tool for lipidomics. *J. Proteome Res.* **2007**, *6*, 552–558.
- (17) Zhao, Y. Y.; Cheng, X. L.; Wei, F.; Bai, X.; Lin, R. C. Application of faecal metabolomics on an experimental model of tubulointerstitial fibrosis by ultra performance liquid chromatography/high-sensitivity mass spectrometry with MS^E data collection technique. *Biomarkers* **2012**, *17*, 721–729.
- (18) Jia, L. W.; Chen, J.; Yin, P. Y.; Lu, X.; Xu, G. W. Serum metabolomics study of chronic renal failure by ultra performance liquid chromatography coupled with Q-TOF mass spectrometry. *Metabolomics* **2008**, *4*, 183–189.
- (19) Zhao, Y. Y.; Liu, J.; Cheng, X. L.; Bai, X.; Lin, R. C. Urinary metabolomics study on biochemical changes in an experimental model of chronic renal failure by adenine based on UPLC Q-TOF/MS. *Clin. Chim. Acta* **2012**, *413*, 642–649.
- (20) Engle, S. J.; Stockelman, M. G.; Chen, J.; Boivin, G.; Yum, M. N.; Daviest, P. M.; Ying, M. Y.; Sahota, A.; Simmondst, H. A.; Stambrook, P. J.; Tischfield, J. A. Adenine phosphoribosyltransferase-deficient mice develop 2,8-dihydroxyadenine nephrolithiasis. *Proc. Natl. Acad. Sci. U.S.A.* **1996**, *93*, 5307–5312.
- (21) Simmonds, H. A.; Sahota, A.; Van Acker, K. J. APRT deficiency: 2,8-dihydroxyadenine lithiasis. In *The metabolic and molecular bases of inherited disease*, 7th ed.; Stanbury, J. B., Wyngaarden, J. B., Fredrickson, D. G., Ed.; McGraw-Hill: New York, 1995.
- (22) Wyngaarden, J. B.; Dunn, J. T. 8-Hydroxyadenine as the metabolic intermediate in the oxidation of adenine to 2,8-dihydroxyadenine by xanthine oxidase. *Arch. Biochem. Biophys.* **1957**, *70*, 150–156.
- (23) De Vries, A.; Sperling, O. Implications of disorders of purine metabolism for the kidney and the urinary tract. *Ciba Found. Symp.* **1977**, *48*, 179–206.
- (24) Yokozawa, T.; Zheng, P. D.; Oura, H.; Koizumi, F. Animal model of adenine-induced chronic renal failure in rats. *Nephron* **1986**, *44*, 230–234.
- (25) Shankland, S. S.; Scholey, J. W.; Thai, K. Expression of transforming growth factor- β 1 during diabetic renal hypertrophy. *Kidney Int.* **1994**, *46*, 430–442.
- (26) Lin, C. Y.; Wu, H.; Tjeerdema, R. S.; Viant, M. R. Evaluation of metabolite extraction strategies from tissue samples using NMR metabolomics. *Metabolomics* **2007**, *3*, 55–67.
- (27) Masson, P.; Alves, A. C.; Ebbels, T. M.; Nicholson, J. K.; Want, E. Optimization and evaluation of metabolite extraction protocols for untargeted metabolic profiling of liver samples by UPLC-MS. *J. Anal. Chem.* **2010**, *82*, 7779–7786.
- (28) Le Belle, J. E.; Harris, N. G.; Williams, S. R.; Bhakoo, K. K. A comparison of cell and tissue extraction techniques using high-resolution ¹H-NMR spectroscopy. *NMR Biomed.* **2002**, *15*, 37–44.
- (29) Ma, C.; Bi, K.; Su, D.; Ji, W.; Zhang, M.; Fan, X.; Wang, C.; Chen, X. Serum and kidney metabolic changes of rat nephrotoxicity induced by Morning Glory Seed. *Food Chem. Toxicol.* **2010**, *48*, 2988–2993.
- (30) McDonald, P. D.; McCabe, D.; Alden, B. A.; Lawrence, N.; Walsh, D. P.; Iraneta, P. C.; Grumbach, E.; Xia, F.; Hong, P. Waters whitepaper, *Topics in liquid chromatography: part 1 designing a reversed-phase column for polar compounds retention* [Online], 2007; <http://www.waters.com/webassets/cms/library/docs/720001889en.pdf>.
- (31) Kaori, K.; Yoshiharu, I.; Ryoko, T.; Atsuko, E.; Kenjiro, M.; Toshimitsu, N. Metabolomic analysis of uremic toxins by liquid chromatography/electrospray ionization-tandem mass spectrometry. *J. Chromatogr., B* **2010**, *878*, 1662–1668.
- (32) Kaori, K.; Yoshiharu, I.; Ryoko, T.; Atsuko, E.; Kenjiro, M.; Toshimitsu, N. Metabolomic search for uremic toxins as indicators of the effect of an oral sorbent AST-120 by liquid chromatography/tandem mass spectrometry. *J. Chromatogr., B* **2010**, *878*, 2997–3002.
- (33) Zhao, Y. Y.; Cheng, X. L.; Wei, F.; Bai, X.; Lin, R. C. Effect of ergosta-4,6,8(14),22-tetraen-3-one (ergone) on adenine-induced chronic renal failure rat: A serum metabolomics study based on ultra performance liquid chromatography/high-sensitivity mass spectrometry coupled with MassLynx i-FIT algorithm. *Clin. Chim. Acta* **2012**, *413*, 1438–1445.
- (34) Zhao, Y. Y.; Shen, X.; Cheng, X. L.; Wei, F.; Bai, X.; Lin, R. C. Urinary metabolomics study on the protective effects of ergosta-4,6,8(14),22-tetraen-3-one on chronic renal failure in rats using UPLC

- Q-TOF/MS and a novel MS^E data collection technique. *Process Biochem.* **2012**, *47*, 1980–1987.
- (35) Gomez Dumm, N. T.; Giannonna, A. M.; Touceda, L. A.; Raimondi, C. Lipid abnormalities in chronic renal failure patients undergoing hemodialysis. *Medicina* **2001**, *61*, 142–146.
- (36) Jia, L.; Wang, C.; Kong, H.; Cai, Z.; Xu, G. Plasma phospholipid metabolic profiling and biomarkers of mouse IgA nephropathy. *Metabolomics* **2006**, *2*, 95–104.
- (37) Jia, L.; Wang, C.; Zhao, S.; Lu, X.; Xu, G. Metabolomic identification of potential phospholipid biomarkers for chronic glomerulonephritis by using high performance liquid chromatography–mass spectrometry. *J. Chromatogr., B* **2007**, *860*, 134–140.
- (38) Yoshioka, Y.; Tsutsumi, T.; Adachi, M.; Tokumura, A. Altered phospholipid profile in urine of rats with unilateral ureteral obstruction. *Metabolomics* **2009**, *5*, 429–433.
- (39) Dyerberg, J. Linoleate-derived polyunsaturated fatty acids and prevention of atherosclerosis. *Nutr. Rev.* **1986**, *44*, 125–134.
- (40) Nakamura, N.; Fujita, T.; Kumakawa, R.; Murakami, R.; Shimada, M.; Shimaya, Y.; Osawa, H.; Hideaki, A.; Okumura, K. Serum lipid profile and plasma fatty acid composition in hemodialysis patients—comparison with chronic kidney disease patients. *In Vivo* **2008**, *22*, 609–612.
- (41) El-Sor, M. H.; Shalaby, H. A. Assessment of the role of polyunsaturated fatty acids in chronic kidney disease. *J. Arab. Soc. Med. Res.* **2010**, *1*, 25–30.
- (42) Baggio, B.; Musacchio, E.; Priante, G. Polyunsaturated fatty acids and renal fibrosis: pathophysiologic link and potential clinical implications. *J. Nephrol.* **2005**, *18*, 362–367.
- (43) Priante, G.; Musacchio, E.; Valvason, C.; Baggio, B. EPA and DHA suppress AngII- and arachidonic acid–induced expression of profibrotic genes in human mesangial cells. *J. Nephrol.* **2009**, *22*, 137–143.
- (44) Niwa, T.; Ise, M. Indoxyl sulfate, a circulating uremic toxin, stimulates the progression of glomerular sclerosis. *J. Lab. Clin. Med.* **1994**, *124*, 96–104.
- (45) Niwa, T.; Ise, M.; Miyazaki, T. An oral sorbent reduces overload of indoxyl sulphate and gene expression of TGF-beta1 in uraemic rat kidneys. *Am. J. Nephrol.* **1994**, *14*, 207–212.
- (46) Miyazaki, T.; Ise, M.; Seo, H.; Niwa, T. Indoxyl sulfate increases the gene expressions of TGF-1, TIMP-1 and pro-1(I) collagen in uremic rat kidneys. *Kidney Int.* **1997**, *52*, S15–22.
- (47) Miyazaki, T.; Ise, M.; Hirata, M.; Endo, K.; Ito, Y.; Seo, H.; et al. Indoxyl sulfate stimulates renal synthesis of transforming growth factor-beta 1 and progression of renal failure. *Kidney Int.* **1997**, *52*, S211–214.
- (48) Martinez, A. W.; Recht, N. S.; Hostetter, T. H.; Meyer, T. W.; Niwa, T. Removal of p-cresol sulfate by hemodialysis. *J. Am. Soc. Nephrol.* **2005**, *16*, 3430–3436.
- (49) Schepers, E.; Meert, N.; Glorieux, G.; Goeman, J.; Van der Eycken, J.; Vanholder, R. p-Cresylsulphate, the main in vivo metabolite of p-cresol, activates leucocyte free radical production. *Nephrol. Dial. Transplant.* **2007**, *22*, 592–596.
- (50) Niwa, T. Indoxyl sulfate is a nephro-vascular toxin. *J. Ren. Nutr.* **2010**, *20*, S2–6.
- (51) Barreto, F. C.; Barreto, D. V.; Liabeuf, S.; Meert, N.; Glorieux, G.; Temmar, M.; Choukroun, G.; Vanholder, R.; Massy, Z. A. Serum indoxyl sulfate is associated with vascular disease and mortality in chronic kidney disease patients. *Clin. J. Am. Soc. Nephrol.* **2009**, *4*, 1551–1558.
- (52) Wikoff, W. R.; Anfora, A. T.; Liu, J.; Schultz, P. G.; Lesley, S. A.; Peters, E. C.; Siuzdak, G. Metabolomics analysis reveals large effects of gut microflora on mammalian blood metabolites. *Proc. Natl. Acad. Sci. U.S.A.* **2009**, *106*, 3698–3703.
- (53) Tsutsumi, Y.; Deguchi, T.; Takano, M.; Takadate, A.; Lindup, W. E.; Otagiri, M. Renal disposition of a furan dicarboxylic acid and other uremic toxins in the rat. *J. Pharmacol. Exp. Ther.* **2002**, *303*, 880–887.
- (54) Taki, K.; Nakamura, S.; Miglinas, M.; Enomoto, A.; Niwa, T. Accumulation of indoxyl sulfate in OAT1/3-positive tubular cells in kidneys of patients with chronic renal failure. *J. Ren. Nutr.* **2006**, *16*, 199–203.
- (55) Toshimitsu, N.; Naohito, T.; Hideo, Y. RNA metabolism in uremic patients: Accumulation of modified ribonucleosides in uremic serum. *Kidney Int.* **1998**, *53*, 1801–1806.
- (56) Young, E. G.; Wentworth, H. P.; Hawkins, W. W. The absorption and excretion of allantoin in mammals. *J. Pharmacol. Exp. Ther.* **1944**, *81*, 1–9.
- (57) Kastenbauer, S.; Koedel, U.; Becker, B. F.; Pfister, H. W. Oxidative stress in bacterial meningitis in humans. *Neurology* **2002**, *58*, 186–191.
- (58) Matrens, M. E.; Storey, B. T.; Lee, C. P. Generation of allantoin from the oxidation of urate by cytochrome c and its possible role in Reye's syndrome. *Arch. Biochem. Biophys.* **1987**, *252*, 91–96.
- (59) Radim, R.; Rubbo, H.; Thomson, L.; Prodanov, E. Luminol chemiluminescence using xanthine and hypoxanthine as xanthine oxidase substrates. *Free Radic. Biol. Med.* **1990**, *8*, 121–126.
- (60) Zinelli, A.; Sotgia, S.; Pisani, E.; Loriga, G.; Deiana, L.; Satta, A. E.; Carru, C. LDL S-homocysteinylation decrease in chronic kidney disease patients undergone lipid lowering therapy. *Eur. J. Pharm. Sci.* **2012**, *47*, 117–123.
- (61) Roman, K.; Pavla, Z. Allantoin as a marker of oxidative stress in human erythrocytes. *Clin. Chem. Lab. Med.* **2008**, *46*, 1270–1274.
- (62) Rahman, A.; Ahmed, S.; Vasenwala, S. M.; Athar, M. Glyceral trinitrate, a nitric oxide donor, abrogates ferric nitrilotriacetate-induced oxidative stress and renal damage. *Arch. Biochem. Biophys.* **2003**, *418*, 71–79.
- (63) Maldonado, P.; Barrera, D.; Medina, C. O.; Hernandez, P. R.; Ibarra, R. M.; Pedraza, C. J.. Aged garlic extract attenuates gentamicin induced renal damage and oxidative stress in rats. *Life Sci.* **2003**, *73*, 2543–2556.